Reports

Microwave Edge Diffraction by Features in Saturn's Rings: Observations with Voyager 1

Abstract. *Classical edge diffraction patterns are formed at centimeter wavelengths by several features of Saturn's rings. These patterns were discovered in 3.6- and 13-centimeter radio signals from Voyager 1 during occultation by the rings. The observed shapes are in agreement with theoretical patterns computed for screens of perfectly abrupt edges having large but finite opacity. Comparison with models in which the opacity at the edge tapers to zero from a finite value sets a new bound of less than about 200 meters on the microwave edge thickness. Certain features of the data suggest a smaller upper bound of about 130 meters on the edge thickness.*

Approximately 3½ hours after its closest approach to Saturn, Voyager 1 passed behind the rings (as seen from the earth) for the purpose of radio occultation studies of the ring structure and particle characteristics (*1, 2*). Strong microwave diffraction effects were observed from the edges of a large number of ring features. This was surprising because diffraction implies sharp transitions of material concentration on the scale of at most a few kilometers in a ring system that spans 280,000 km. We know of no a priori suggestions that such sharp transitions would be present. However, such features were observed to be common throughout the ring system. We report here results on diffraction for the Encke gap [~ 2.21 Saturn radii (R_S); Fig. 1] and the outer edge of ring A, including the small gap discovered by Voyager 1 about 250 km interior to the edge of ring A (~ 2.26 R_S; Fig. 2). Comparison of the observed diffraction with patterns calculated from models of the edge leads to new limits on the microwave thickness of the edge.

At the time of these observations Voyager 1 was at a distance $D \cong 215{,}000$ km behind the rings and moving 21.3 km/sec with respect to Saturn; its component of velocity in the plane of the sky perpendicular to the projection of the rings at the points of interest was 8.8 km/sec. The data consisted of high-rate samples of spacecraft transmissions at wavelengths (λ) 3.6 and 13 cm received by the NASA Deep Space Network 64-m-diameter antenna facility near Madrid, Spain. Only the 3.6-cm observations are discussed here; similar results were obtained at the longer wavelength but at lower signal-to-noise ratios. The data were filtered to obtain the power (or intensity) in the coherent or "direct" component of the wave passing through the rings, excluding near-forward scattering by ring particles, which was also observed in the power spectra of the received signal as a Doppler-broadened feature surrounding the coherent wave (*3*). Because the time of the Voyager 1 encounter was only slightly past the equinox for Saturn, the rings were only partially open, with an angle between the radio path and the ring plane of $\xi = 5.9°$. Thus the length of the radio path through the rings was 9.7 times its value at right angles to the rings for both the physical and optical distances (*4*). This high obliquity of the rings also affected the diffraction geometry. At $\lambda = 3.6$ cm the Fresnel zone size was $\sqrt{\lambda D/2} \simeq 1.97$ km measured at the rings in a plane perpendicular to the radio path. When corrected for projective effects, the effective Fresnel zone in the neighborhood of the edge of ring A was 15.2 km measured along the radial direction from Saturn in the ring plane.

The results shown give one example of edge diffraction (Fig. 2b, outer edge of ring A), one distinct example of slit diffraction (Fig. 2a, narrow gap inside ring A), and one example of an intermediate result (Fig. 1, Encke gap), where the effects of two edges of a slit are well separated.

Measurements of coherent signal intensity passing through the rings interior and exterior to the Encke gap yielded finite values for the oblique 3.6-cm microwave opacity of the rings of approximately $\tau(3.6 \text{ cm}) \simeq 6.5$ and 7.5 at these

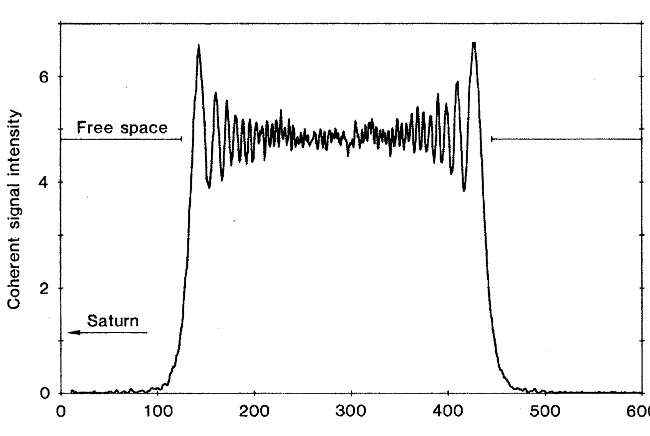

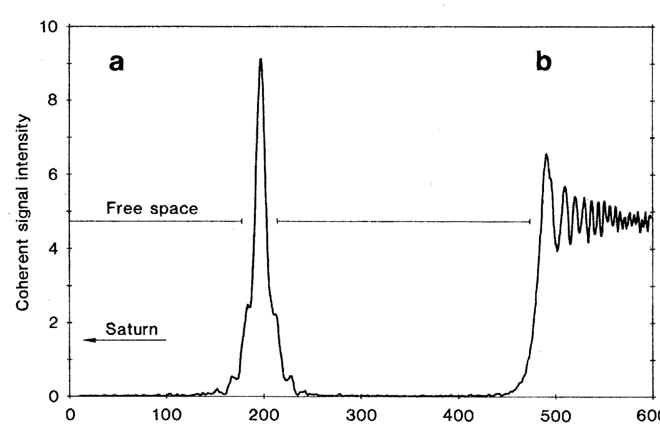

Fig. 1 (left). Diffraction by the Encke gap at $\lambda = 3.6$ cm observed as variations in coherent signal intensity (*3*) received on the earth as Voyager 1 passed 215,000 km behind the gap. Oscillations about the estimated free-space signal level result from edge diffraction at the inner and outer boundaries of the gap, which are inferred to be ~ 21.1 Fresnel zones (320 km) apart. The break in the horizontal line labeled "Free space" corresponds to the estimated width and location of the gap. Weak signal levels near the baseline correspond to transmission through adjacent regions of ring A. Data points were computed each 600-m radial distance in ring plane but are shown smoothed over a 2.4-km interval. Fig. 2 (right). Diffraction at 3.6 cm by outer ring A. (a) Sharp narrow feature corresponding to small gap discovered by Voyager 1. Its width is ~ 2.45 Fresnel zones (37 km). (b) Outer edge of ring A. Breaks in the horizontal line labeled "Free space" indicate the estimated widths and location of the gap and the location of the edge of ring A.

 0036-8075/82/0716-0243$01.00/0

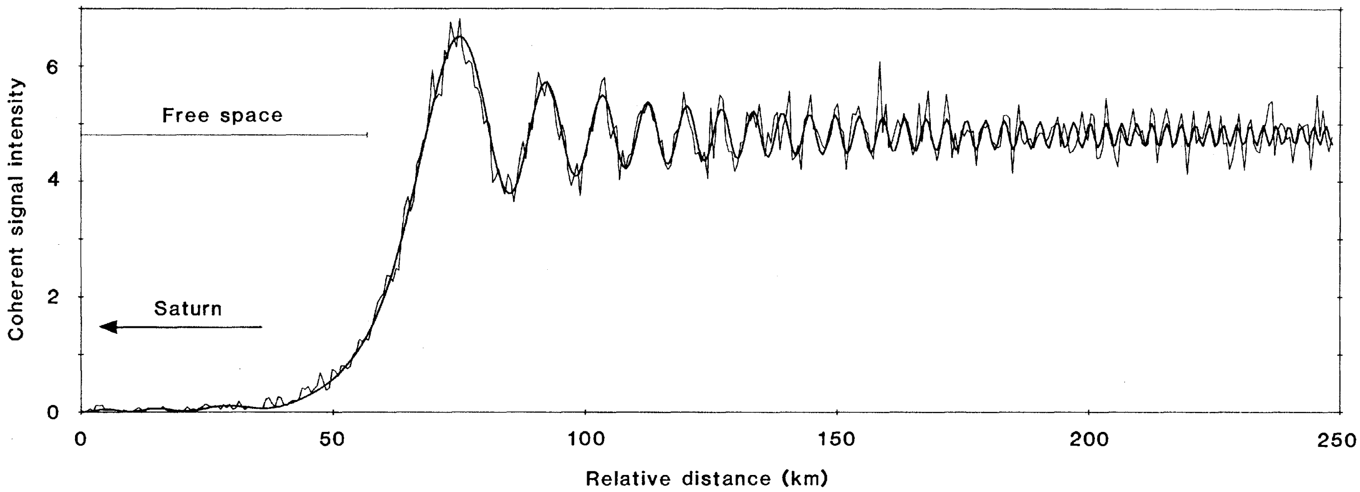

Fig. 3. Comparison of theory with observation for the inner edge of the Encke gap. Smooth curve is theoretical diffraction from an abrupt edge of a gray screen with opacity 6.5; fluctuating curve corresponds to the left-hand portion of the curve from Fig. 1, but plotted here at each 600 m of radial distance in the ring plane. Horizontal scale of theoretical curve is based on experimental geometry; vertical scale and right-left position are obtained by least-mean-squares fitting to the data. Patterns match for about 30 oscillations, although an intermediate discontinuity can be seen after about 20 oscillations. The last few oscillations may be due to the outer edge of the gap.

locations, respectively, where the transmitted intensity varied as $\exp[-\tau(3.6\ \text{cm})]$. The value for τ exterior to Encke gap is also appropriate to the region of the smaller gap and the edge of ring A. We interpret the associated diffraction patterns given in Figs. 1 and 2 as resulting from a sharp change in the opacity, from the values just given to $\tau = 0$.

In the vicinity of these edges the rings appear to first order to act as opaque screens, although they are more properly described as "gray" screens, which transmit about 0.00055 to 0.0015 of the incident intensity, rather than the totally absorbing "black" screen usually employed in physical optics theories.

The curve of Fig. 1 for the Encke gap corresponds in considerable detail to the theoretical diffraction pattern of a slit in an opaque screen 21.1 Fresnel zones ($\simeq$ 320 km) in width. The principal deviations from the theoretical pattern occur near the center, where interference effects from the two edges are most important and small deviations from the theoretical edge would be expected to be of greatest significance. In addition, Voyager 2 images of the rings at high emission angles showed the Encke gap to contain narrow, irregular ringlets, which may have affected the results in the central portion of the gap (*5*).

The outer ring A gap (Fig. 2a) shows another aspect of slit diffraction. In this case the intensity reaches a peak value 1.98 times the free-space level, while the base of the pattern shows clear shoulders. These features are well matched by diffraction from a slit in an opaque screen 2.45 Fresnel zones ($\simeq$ 37 km) in width. However, there are significant differences between the theoretical curve for this case and the ring observation. For example, the theoretical curve that best matches the shoulders falls below the peak by 9 percent. Also note the slight asymmetry of the observational result.

Figure 2b shows the result for the outer edge of ring A. Here, about nine oscillations of the curve are clearly visible.

Comparison of the patterns for these and other locations with theoretical models for the variations in opacity near the edge yields variable results, but the agreement between the observations and simple models can be quite good. Figure 3 shows, as one example, a comparison of the signal from the interior edge of the Encke gap with diffraction from the edge of a screen of opacity $\tau(3.6\ \text{cm}) = 6.5$. The shape of the theoretical curve is based entirely on the geometry of the Voyager experiment and physical optics theory, while the vertical scale and right-left position have been adjusted for best mean-squares fit. Notice the agreement for the approximately 30 oscillations shown. The small oscillations near the left end of the observations are characteristic of the finite opacity of the screen and are not present in diffraction by completely opaque screens.

Comparisons with theoretical models in which the opacity at the edge of the screen varies linearly from 6.5 to 0.0 over finite widths indicate that the observations cannot be matched for transition distances greater than about 0.1 Fresnel zone, or about 1.5 km in the radial dimension in the ring plane. Thus 1.5 km is an upper bound for the radial distance of transition in microwave opacity for this feature. If one considers a slab model of finite thickness for the rings, in which the edge is blunt in the radial dimension, then the limits above can be combined with the highly oblique angle of the ray to the ring plane to obtain a bound on the physical thickness of the edge (*6*). The result is that the thickness at the edge is less than about 200 m, as a strong upper bound.

A different line of argument leads to lower values for the bound on edge thickness, however. We commonly observe a fine structure in the intensity curves on spatial scales corresponding to about 1 km in radial distance. This can be seen in Fig. 3 as short-period oscillations superimposed on the first few cycles of the diffraction pattern. If these oscillations are due to the diffraction tails of other edges, then as a consequence of the behavior of the higher order Fresnel zone pattern, such edges must be sharp on about the same spatial scale as the period of the observed oscillations. A 1-km edge taper distance translates to a bound on edge thickness of approximately 130 m. However, high-frequency fluctuations on the above scale could also be caused by interference effects from distant gaps that are narrow on the scale of the Fresnel zone.

Diffraction effects in the rings are not limited to the examples given in Figs. 1 and 2, but occur in perhaps a dozen locations within rings A and C and the Cassini division (*7*). They are usually, but not always, associated with a transition from large but finite opacity to nearly zero opacity. Prominent examples of diffraction occur at the outer edges of rings A (Fig. 2) and B, at the edges of the eccentric ring ($\simeq 1.446\ R_S$), near all gaps within the Cassini division and ring A, and even at ring F. No diffraction is observed at the interface between rings B and C or between the interior of ring A and the bright outer band of the Cassini division discovered by Pioneer 11 at $\simeq 2.01\ R_S$. This variation in the character of the edges may reflect variations in the underlying mechanisms responsible for their formation. However, the fact that features exhibiting edge diffraction occur over the inner and outer parts of the rings suggests a common causal process throughout the ring system.

On the basis of the wavelength employed, these results apply to particles in the rings with diameters greater than about 1 cm. Particles substantially smaller than 1 cm are in the Rayleigh scattering regime at $\lambda = 3.6$ cm and are probably of little importance in the intensity measurements considered here (*8*).

Estimates of the edge thickness based on ring occultation of the star δ-Scorpii were reported by the Voyager photopolarimeter experiment team (*9*). The characteristic bound obtained was about 125 m, which is consistent with the bounds reported here. These results complement one another in that they apply to different ranges in the particle size distribution. Optical extinction measurements apply to the collection of particles larger than about 2×10^{-7} m, whereas the radio results apply to the collection of particles larger than about 1×10^{-2} m. Since the stellar and radio occultations were obtained at different times and different geometries, they do not necessarily refer to the same characteristic of the edge. For example, a thin sheet of small particles could extend beyond the edge defined by the radio occultation, yielding the same thickness results for the two experiments, but without coincidence between the location of the discontinuity at optical and microwave wavelengths.

The radio occultation data also contain information on the variations of the phase of the complex coherent signal whose intensity was used to compute the diffraction patterns presented above. In effect, the coherent data correspond to a one-dimensional sampling of the microwave hologram formed behind the rings. By use of an inverse Fresnel transform it may be possible to obtain a more precise measure of edge characteristics than can be inferred by modeling.

ESSAM A. MAROUF
G. LEONARD TYLER
*Center for Radar Astronomy,
Stanford University,
Stanford, California 94305*

References and Notes

1. The Voyager radio science ring occultation experiment is described by V. R. Eshleman, G. L. Tyler, J. D. Anderson, G. Fjeldbo, G. S. Levy, G. E. Wood, and T. A. Croft [*Space Sci. Rev.* **21**, 207 (1977)]; preliminary results are given by G. L. Tyler, V. R. Eshleman, J. D. Anderson, G. S. Levy, G. F. Lindal, G. E. Wood, and T. A. Croft [*Science* **212**, 201 (1981)].
2. The theory of radio occultation by planetary rings is given by E. A. Marouf, G. L. Tyler, and V. R. Eshleman [*Icarus* **49**, 161 (1982)].
3. Waves propagating through the rings can be separated into coherent and incoherent components, corresponding to deterministic or random behavior of the signal phase. The coherent and incoherent waves correspond to the direct (or reduced) and scattered (or diffuse) waves of radiative transfer theory [S. Chandrasekhar, *Radiative Transfer* (Dover, New York, 1960)]. We use the term coherent to emphasize the monochromatic nature of the experiment, which is not usually important in related optical scattering observations. Experimentally, the two components were readily distinguished on the basis of differential Doppler effects. The coherent wave was essentially unchanged in frequency from the value expected on the basis of the spacecraft motion with respect to the earth receiving station. Scattered signals, however, generally undergo an additional Doppler shift as a result of interaction with moving particles that are not along the geometric line of sight. This separation of components for radio occultations by rings is discussed in E. A. Marouf, thesis, Stanford University (1975) and in (*2*).
4. The rings are assumed to consist of a many-particle-thick differentially rotating slab of material that can be described in terms of average loss and scattering coefficients per unit volume. For this assumption, the minimum thickness must be many wavelengths. Estimates of the volumetric packing of the rings are in the range 10^{-3} to 10^{-2} [M. S. Bobrov, in *Surfaces and Interiors of Planets and Satellites*, A. Dollfus, Ed. (Academic Press, New York, 1970), pp. 377–458] and are consistent with this model.
5. The Voyager imaging team reported at least two narrow irregular ringlets within the Encke gap [B. A. Smith *et al.*, *Science* **215**, 504 (1982)]. These ringlets could also produce coherent diffraction, which would perturb the overall pattern formed by the edges acting alone.
6. An oblique ray that enters or exits the ring through a blunt edge will not experience the full opacity of the slab. This will cause the transition from the opacity of the slab to that of free space to occur over a finite transition width W, causing the edge to appear less sharp. The width W depends on the inclination angle ξ of the line of sight to the ring plane and the angle Ψ between the edge and the projection of the line of sight on the ring plane. An upper bound on slab thickness T in the vicinity of the edge is then $T \lesssim W \tan \xi / \cos \Psi$. The results reported here correspond to $\Psi \simeq 36°$ and $\xi = 5.9°$.
7. Ring B is excluded from this list. Typical values for the oblique microwave opacity in ring B exceed $\tau \sim 10$. We cannot obtain the necessary time resolution to observe diffraction from ring B features at the much lower signal-to-noise ratios obtained for ring B. Adequate signal-to-noise ratios would be achieved for a similar experiment at larger ring openings.
8. The importance of the small particles depends on the size distribution. Particles more than about 1 cm in diameter remove energy from the $\lambda = 3.6$ cm coherent wave in proportion to their areas; particles in the Rayleigh regime remove energy as area cubed. For power-law size distributions with index greater than about −4, the effects of particles less than about 1 cm in diameter can be neglected.
9. A. L. Lane *et al.*, *Science* **215**, 537 (1982).
10. We thank V. R. Eshleman for several useful and illuminating discussions and our colleagues at Stanford, in particular R. A. Simpson, M. Plume, H. Zebker, F. Orabona, and L. W. Raley, for their efforts in reducing the ring occultation data. We thank the members of the Voyager Project, the members of the radio science team, and the members of the radio science support team at Jet Propulsion Laboratory for support during the planning, implementation, execution, and data acquisition phases of the experiment. This work was supported by the Planetary Atmospheres Program of the National Aeronautics and Space Administration and by Jet Propulsion Laboratory.

22 March 1982; revised 24 May 1982

Advection of Pore Fluids Through Sediments in the Equatorial East Pacific

Abstract. *Measurements of the ratio of helium-4 to helium-3 and of calcium ion in the pore waters of sediments at two locations in the eastern equatorial Pacific indicate that solution advection is occurring through the sediments. Both the helium ratio and the calcium ion profile yield velocity values for advective flow of about 20 centimeters per year. Mass balance constraints are also consistent with the interpretation presented. Flow appears to be occurring through relatively thick sediments, on the order of 300 meters.*

The subject of slow advective flow of solutions through marine sediments has received considerable attention over the past several years. Most discussions presented so far have been based upon interpretations of temperature profiles, with flow being determined from nonlinear temperature gradients in the absence of corresponding changes in thermal conductivity (*1, 2*). Advection consistent with thermal measurements also has been inferred from pore water Ca^{2+} profiles in relatively thin sediments (*3*). The case for advection in thick (> 100 m) sediments is, however, controversial, with chemical corroboration of flow based upon temperature profiles lacking. In the one case where chemical and thermal data were collected simultaneously, discordant results were obtained, the chemical data (SO_4^{2-}) indicating little if any flow (*4*). In addition, velocities estimated from thermal data often are inconsistent with reasonable values of permeability, the hydrostatic head required to produce the estimated velocity being sufficient to "lift" the sediment overburden.

Characterization of the occurrence and nature of fluid flow through sediments is important from both a geochemical and a geophysical point of view. Such flow could provide a hitherto ignored conduit between the crust and the overlying ocean water, influencing heat transfer and the geochemical budgets of

0036-8075/82/0716-0245$01.00/0